Int. J. Electrochem. Sci., 3 **(2008)** 67 - 74

International Journal of ELECTROCHEMICAL SCIENCE
www.electrochemsci.org

Hydrothermal Synthesis and Electrochemical Characterization of α-MnO_2 Nanorods as Cathode Material for Lithium Batteries

Yanyan Yang, Lifen Xiao[*]*, Yanqiang Zhao and Fengyun Wang*

College of Chemistry, HuaZhong Normal University, Wuhan 430079, China
[*]E-mail: lfxiao@mail.ccnu.edu.cn

Received: 30 October 2007 / *Accepted:* 07 November 2007 / *Online published:* 20 November 2007

One dimensional(1-D) α- MnO_2 nanorods with diameters of 10～20nm are directly prepared by hydrothermal treatment of γ- MnO_2. When used as lithium intercalation cathode, the α- MnO_2 nanorods have delivered specific capacity of 220, 189 and152mAh/g at the current of 10, 50, and 100mA/g respectively. Also, the nanorods have exhibited quite good cycling stability with a cycling capacity of 130mAh/g after the 25th cycle. The results demonstrated a possible use of the α-MnO_2 nanorods as a competitive cathode material for rechargeable lithium battery.

Keywords: α- MnO_2 nanorod; hydrothermal; rechargeable lithium battery

1. INTRODUCTION

Manganese dioxide is an important battery material extensively used as air cathode catalyst [1,2], cathode materials for aqueous primary batteries and nonaqueous rechargeable lithium batteries [3,4]. Particularly, manganese oxides are considered to be a most attractive candidate as cathodic materials for the next generation of lithium ion because of its abundant natural resources, low-cost and environmental friendliness.

Electrochemical properties of MnO_2 depend strongly on the crystalline structure and morphology of the oxide. It has been well known that the manganese dioxides exist in various polymorphic forms concluding α-, β-, γ- and δ- MnO_2, which are different in the spatial arrangement of basic octahedral [MnO_6] units. Among the all of these manganese dioxides, α-MnO_2 have now received special attention as cathode materials for lithium batteries [5], since the large 2×2 tunnels existing in the crystalline lattice of α-MnO_2 are believed to facilitate the accommodation and transportation of inserting lithium ions.

It is well accepted that the kinetics of a Li^+ intercalation process is controlled predominately by the diffusion rate of Li^+ ion in the solid-phase of MnO_2, which determines the electrochemical performance of the MnO_2 cathode. Nanosized materials have higher active surface area and smaller diffusion length for the Li^+ intercalation, and therefore should have higher specific capacity and better rate capability than the large size particles. Materials with 1-D nano structure not only have sufficiently high surface area and short distance from surface to interior core, but also have smallest dimension, which will provide more effective electrical transport continuity and minimize lithium-ion diffusion path. Based on this consideration, there has been increasing interest recently in the fabrication of one-dimensional nano-MnO_2, such as MnO_2 nanowires [6-9] and nanorods [9-12]. For example, X. Wang, et al. [7,10] have reported the synthesis of 1-D α-MnO_2 single-crystal nanowires and nanorods in a hydrothermal method through the oxidation of $MnSO_4$ by $(NH_4)_2S_2O_8$ or $KMnO_4$ respectively. Q. Li, et al. [6] have synthesized well-aligned α-MnO_2 nanowires by electrochemical step-edge decoration. Also, α-MnO_2 nanorods with uniform diameter were obtained by M. Sugantha, et al. through a sol-gel synthetic route [11].

Hydrothermal method is a simple and feasible method to prepare one-dimensional nanoscaled materials. As the crystal growth is anisotropic, it is prone to grow slowly toward one-dimensional direction under the hydrothermal conditions such as high pressure and temperature. In the present work, we found that γ- MnO_2 can spontaneously transform into α-MnO_2 nanorods in a hydrothermal condition. This paper reports the structure and morphology of the α-MnO_2 nanorods produced by such a hydrothermal reaction and the performance characteristics of this material used as lithium intercalation cathode.

2. EXPERIMENTAL PART

All chemical reagents used in this work were of analytical grade. The H_2O_2 solution (1:10, molar ratio of H_2O_2 to distilled water) was added dropwise into 0.01M $KMnO_4$ solution at continuous stirring till the $KMnO_4$ has just completely reduced, which was monitored by the disappearance of the purple color of $KMnO_4$. The redox reaction leads to gelatinous precipitate. The precipitate was subsequently tendered with dense HNO_3, and then filtered, washed with dilute HNO_3 solution and distilled water, and finally dried at 80^{o}C. The final product is marked as chemically synthesized MnO_2 (CMD). The CMD was transferred into a Teflon-lined stainless steel autoclave, which was filled with distill water up to 90% of total volume. Then the autoclave was sealed and maintained at 120 ^{o}C for 12h. After the reaction was complete, the autoclave was cooled down naturally to room temperature. Then the resulting brown precipitate was further filtered and washed with distilled water, and finally dried at 80 ^{o}C. The product as treated is marked as hydrothermal-treated MnO_2 (HMD).

The crystalline structures of the MnO_2 powders were characterized using an X-ray diffraction (Shimadzu XRD-6000 diffractometer with Cu Kα) and a Scanning Electron Microscope (JEOL JSM-6700F).

The charge-discharge properties were measured on the test cells of a three-electrode design. The MnO_2 cathodes were prepared by roll-pressing the mixed paste of 80% MnO_2 powder, 8%

acetylene black and12% PTFE (wt.%) into ca. 100μm thick film and then pressing the electrode film onto a nickel net. The counter electrodes and reference electrodes were lithium sheets. The separator was Celgard 2400 microporous membrane. The electrolyte was 1M $LiPF_6$ dissolved in a 1:1:1 mixture (by weight) of ethylene carbonate (EC), dimethyl carbonate (DMC) and ethylene methyl carbonate (EMC) purchased from Shinestar battery materials co., Ltd (China). The cells were assembled in an argon-filled glove box. The charge-discharge measurements were carried out using a battery charger between 1.5 to 4.3V vs. Li/Li^+.

3. RESULTS AND DISCUSSION

Fig.1 compares the XRD patterns of the CMD and HMD samples. As can be seen, all the diffraction peaks of CMD are in good agreement with the standard values of γ-MnO_2 (JCPDS 14-0644), indicating that the CMD has an γ-MnO_2 structure. Traditionally, γ-MnO_2 is synthesized by the chemical reduction of $KMnO_4$ in the presence of H_2O_2. As also shown in Fig.1, all the diffraction lines of the HMD exactly belong to α-MnO_2 (JCPDS 44-0141), suggesting that pure α-MnO_2 can be obtained through hydrothermal treatment. The comparison of the patterns in Fig.1 thus reveals a crystal structural transformation from γ-phase to α-phase occurring on MnO_2 during hydrothermal treatment. At first glance, it may be surprising to see this phenomenon because γ- and α-MnO_2 is quite different. γ-MnO_2 is considered to be random intergrowth of 1×1tunnels of pyrolusite and 2×1 tunnels of ransdellite constructed of octahedral [MnO_6] unit [13] while α-MnO_2 is made up of double chains of

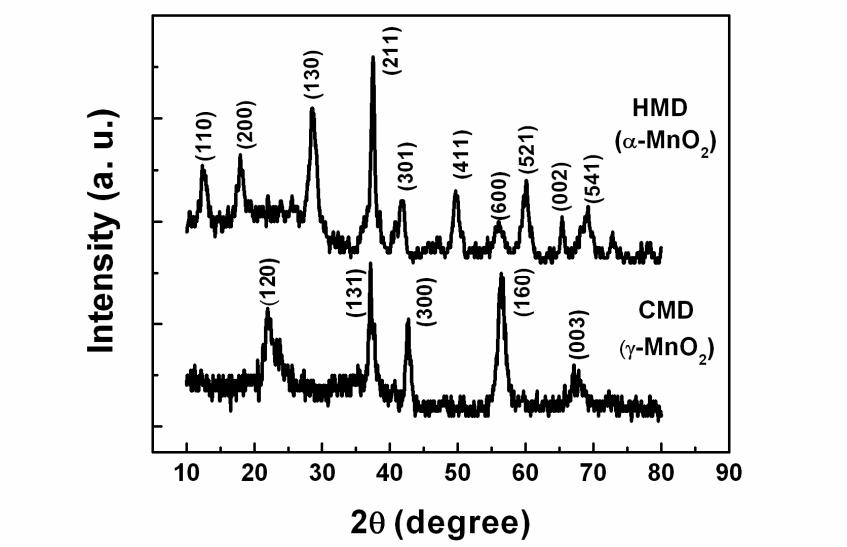

Figure 1. XRD powder patterns of CMD and HMD.

[MnO_6] octahedral forming 2×2 and 1×1 tunnels [14]. The reasonable explanation of this phenomenon, we believe, is that the starting γ-MnO_2 is firstly dissolved to form a saturation solution and then α-MnO_2 gradually crystallizes from the solution in the hydrothermal environment (relatively high pressure and temperature). During the crystalline phase transformation from γ-MnO_2 to α-MnO_2, water

molecules must play an important role because distill water was found to be a favorable solvent for this hydrothermal reaction in our experiments. As reported in previous work [15], H_2O had been accommodated within the 2×2 tunnel of α-MnO_2 and acted as stabilizing molecules necessary for building up the framework structure of the 2×2 tunnels. Other works as mentioned above also indicated that a hydrothermal environment facilitates very well the growth of α-structured MnO_2 [7-10,12].

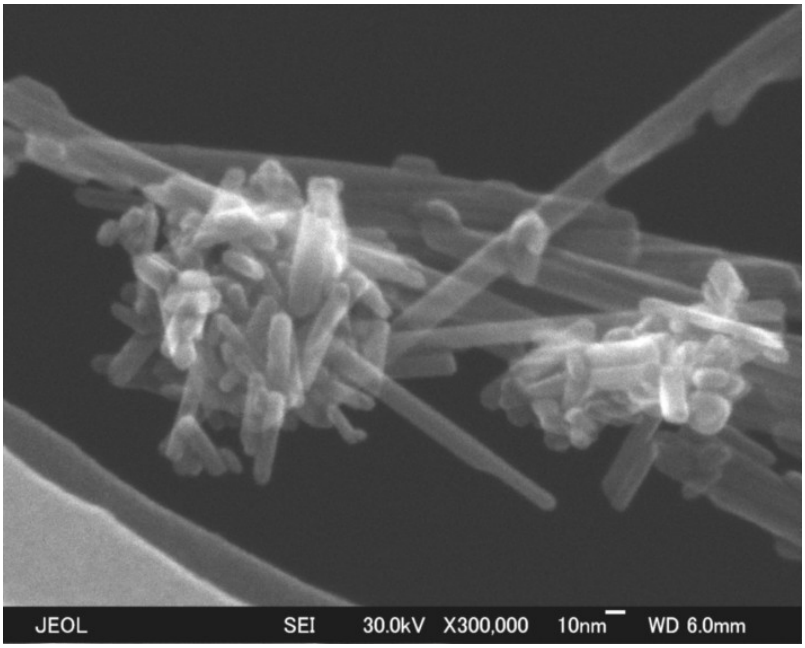

Figure 2. SEM photograph of the as-synthesized α-MnO_2(HMD).

The morphology of the α-MnO_2 sample as synthesized is showed in Fig.2. It is clearly shown that the product is made up of nanorods with a diameter of approximately 10～20nm, but the lengths of nanorods are quite uneven and of the order of several tens of nanometers to several micrometers. The SEM image also confirms the phenomenon that α-MnO_2 tends to form low dimensional crystal under the hydrothermal conditions as reported in previous literature. Owing to its special structure, the as-synthesized 1-D nanosized MnO_2 should exhibit better electrochemical performance such as intercalation capacity and discharge rate than commonly used MnO_2 powders.

To evaluate the electrochemical behaviors of the as-synthesized 1-D α-MnO_2 nanorods, we used the simulated Li/MnO_2 cells to characterize the charge-discharge performances. Fig.3 shows the initial discharge curves of the as-synthesized α-MnO_2 at the discharge current of 50mA/g as well as CMD and commercial EMD for comparison. As can be seen, the as-synthesized α-MnO_2 can deliver a discharge capacity of 189mAh/g, much larger than that of CMD (134mAh/g) and EMD (148mAh/g). This phenomenon can be well accounted for by the fact that nanorods of the as-synthesized MnO_2 have only one dimensional geometry and a much larger surface area than that of three dimensional micrometer CMD and EMD powders, resulting in a shortening of the diffusion path of lithium ion in the solid phase of the materials, and therefore helping to improve the spatial utilization of materials.

Fig.3 also shows that there is an insignificant reduction of the discharge voltage profile for the as-synthesized α-MnO_2 at the experimental conditions as compared with CMD and EMD. This phenomenon is probably due to the thermodynamic factors for Li^+ intercalation brought about by the different crystalline structures of the MnO_2 materials. From the XRD data in Fig.1, the CMD has γ-type structure similar to that of commercial EMD, so they displayed the same discharge voltage profile as EMD, while the HMD has α-type structure and behaves like α-MnO_2 as suggested in previous work [16], showing a discharge voltage at about 2.6V.

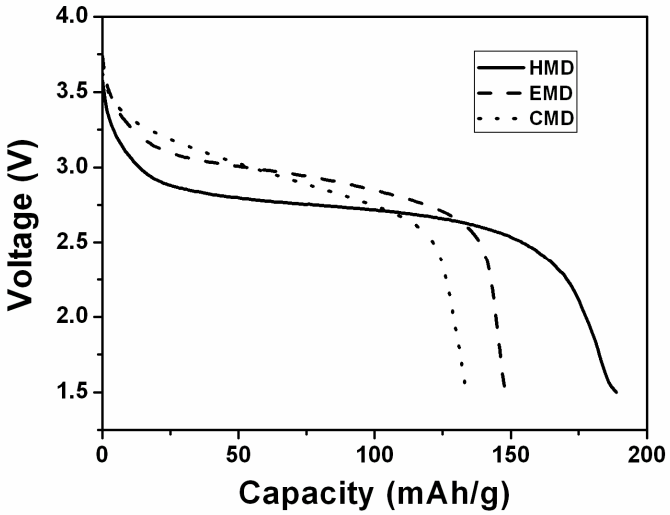

Figure 3. A comparison of the first discharge curves of the α-MnO_2 nanorod (HMD) , CMD and commercial EMD at 50mA/g.

To evaluate the cycling performance of the α-MnO_2 nanorods, the test cells were cycled at voltage interval of 1.5V～4.3V at constant current of 50mA/g. The capacity curves at first 25 cycles are shown in Fig.4. The results demonstrated that both CMD and EMD display rapid capacity fading throughout the cycles and loss most of their capacity after the 20th cycle (only about 40mAh/g left). This poor cycling performance mainly arise from the fact that the γ-MnO_2 usually undergoes an irreversible phase transformation to spinel structure during cycling, which brings a large capacity loss. The as-prepared α-MnO_2 nanorods also presented a capacity loss in the initial four cycles (about 41mAh/g from the initial 189mAh/g to 148mAh/g at the 4th cycle). This capacity loss is probably due to the fact that a fraction of lithium ions inserted during the initial discharge become locked within the crystal structure of MnO_2 for lattice stabilization. However, the material subsequently exhibits excellent cycling stability. After the 25th cycle, the nanorods can still deliver a capacity of 130mAh/g, which is much better than that of CMD and EMD. The cycling stability of α-MnO_2 nanorods electrode should be attributed to its special geometry and morphology. Compared to commonly used CMD and EMD powders, this special column-shaped-nanorod structure with short diameter would decrease the structure stress during lithium ion intercalation and deintercalaction, which results from lithium ion diffusion and electron transfer in MnO_2 crystal structure. Furthermore, the additional water molecules within the 2×2 tunnels of α-MnO_2 structure may also help the α-MnO_2 framework maintain stable

towards lithium insertion and extraction and therefore suppress the capacity fade of the materials during cycling.

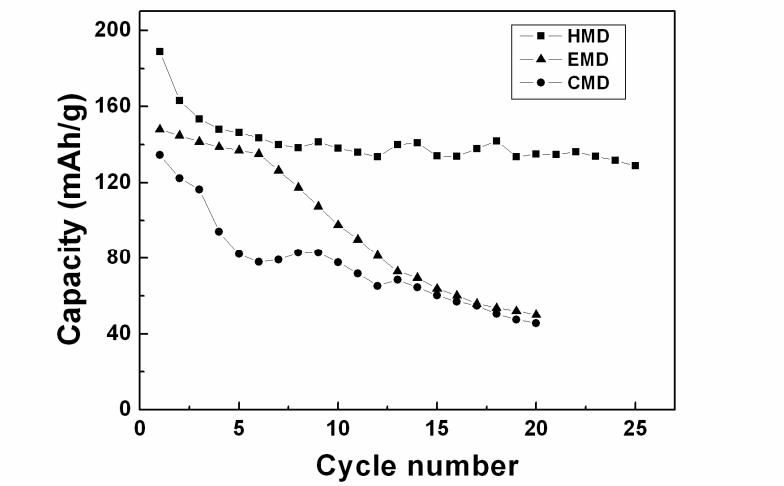

Figure 4. A comparison of the cycling performances of the α-MnO_2 nanorod (HMD), CMD and EMD at 50mA/g.

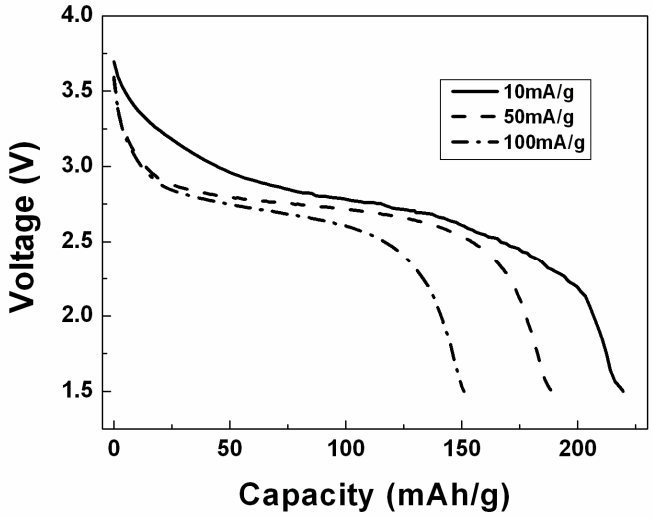

Figure 5. The discharge curves of the α-MnO_2 nanorodes (HMD) at different current rates.

Fig. 5 shows the rate capability of as-prepared α-MnO_2 at three different current densities, 10mA/g, 50mA/g, and 100mA/g. At the lower current rate of 10mA/g, the nanorods exhibit a quite high discharge capacity of 220mAh/g and most of lithium intercalation capacity occurs at higher voltage ≥ 2.5V. When the current density was increased to 50mA/g and 100mA/g, the initial discharge capacity reduced to189mAh/g and152mAh/g, which is approximately 84% and 69% of the capacity observed at lower current density of 10mA/g. It is recognized that Li^+ ions diffusion in the solid phase of the active material is usually the rate-limiting step in the intercalation reaction. Therefore, the

discharge current density can severely affect the discharge capacity of MnO_2 electrode. However, there is still a considerable high capacity delivered for α-MnO_2 nanorods at 100mAh/g, demonstrating a quite good rate performance of this material. As mentioned above, the 1D-nano structure can minimize the diffusion length while the larger 2×2 tunnels of α-MnO_2 structure can enhance the diffusion rate. Compared with the previous literature [17,18], the as-prepared MnO_2 nanorods electrode can deliver better rate capability. This is indeed because the nanorods synthesized by our method have uneven and decreased diameter (about 10~20nm), and therefore this material can provide a short diffusion path of lithium ion, alleviating the diffusive resistance of Li^+ intercalation reaction. In a word, these electrochemical data strongly suggest the as prepared MnO_2 nanorods are very promising as cathode material for rechargeable lithium batteries.

4. CONCLUSIONS

One dimensional α-MnO_2 nanorods can be synthesized by hydrothermal treatment of γ- MnO_2 prepared though the reaction of $KMnO_4$ and H_2O_2. When used for lithium intercalation electrode, the material can improve not only the initial discharge capacity, but also the cycling stability during subsequent cycles. Furthermore, the α-MnO_2 nanorods have an improved rate capability than those previously reported. Since the hydrothermal procedure is simple and effective, this material may have potential applications for rechargeable lithium battery.

ACKNOWLEDGMENTS
This research was financially supported by the National 973 Program of China (No. 2002CB211800) and National Science Foundation of China (No. 50502025).

References

1. L. Mao, T. Sotomura, K. Nakatsu, N. Koshiba, D. Zhang, and T. Ohsaka, *J. Electrochem. Soc.* 149 (2002) A504
2. Y. L. Cao, H. X. Yang, X. P. Ai, L. F. Xiao, *J. Electroanal. Chem.* 557 (2003) 127
3. F. Cheng, J. Chen, X. Gou, P. Shen, *Adv. Mater.* 17 (2005) 2753
4. J. J. Xu, H. Ye, G. Jain, J. Jang, *Electrochem. Commun.* 6 (2004) 892
5. A. M. Morales and C. M. Lieber, *Science* 279 (1998) 208
6. Q. Li, J. B. Olson and R. M. Penner, *Chem. Mater.* 16 (2004) 3402
7. X. Wang and Y. Li, *J. Am. Chem. Soc.* 124 (2002) 2880
8. Y. Gao, Z. Wang, J. Wan, G. Zou, Y. Qian, J*ournal of Crystal Growth* 279 (2005) 415
9. Y. Liu, M. Zhang, J. Zhang and Y. Qian, *Journal of Solid State Chemistry* 179 (2006) 1757
10. X. Wang and Y. Li, *Chem. Commun.* (2002) 764
11. M. Sugantha, P. A. Ramakrishnan, A. M. Hermann, C. P Warmsingh and D. S. Ginley, *International Journal of Hydrogen Energy* 28 (2003) 597
12. R.Yang, Z. Wang, L. Dai, and L. Chen, *Materials Chemistry and Physics* 93 (2005) 149
13. Y. Chabre and J. Pannetie, *Prog. Solid State Chem.* 23 (1995) 1
14. M. M. Thackeray, *Prog. Solid State Chem.* 25 (1997) 1
15. Ph. Botkowitz, R. Brec, Ph. Deniard, M. Tournoux; G. Burr, *Mol. Cryst. Liq. Cryst.* 244 (1994) 233

16. Y. L. Lu, M. Wei, Z. Q. Wang, D.G. Evans and X. Duan, *Electrochimica Acta* 49 (2004) 2361
17. V. G. Kumar, J. S. Gnanaraj, G. Salitra, A. Abramov, A. Gedanken, D. Aurbach, J. B. Soupart, J. C. Rousche, *J. Solid State Electrochem.* 8 (2004) 957
18. L. I. Hill, A. Verbaere, D. Guyomard, *J. Power Sources* 119-121 (2003) 226